International Journal for Innovative Engineering and Management Research
PEER REVIEWED OPEN ACCESS INTERNATIONAL JOURNAL
www.ijiemr.org

COPY RIGHT

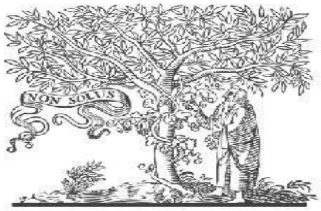

ELSEVIER SSRN

IJIEMR Transactions, online available on 26th Nov 2022. Link :http://www.ijiemr.org/downloads.php?vol=Volume-11&issue=Issue 11

10.48047/IJIEMR/V11/ISSUE 11/58

TITLE: A STUDY OF MAGNETIC FILLER'S IMPACT ON PEDOT/GRAPHENE COMPOSITE
Volume 11, ISSUE 11, Pages: 463-473

Paper Authors **E ASHOK SIVA KUMAR, Dr. Satish Kumar**

USE THIS BARCODE TO ACCESS YOUR ONLINE PAPER

To Secure Your Paper As Per UGC Guidelines We Are Providing A Electronic Bar Code

International Journal for Innovative Engineering and Management Research
PEER REVIEWED OPEN ACCESS INTERNATIONAL JOURNAL
www.ijiemr.org

A STUDY OF MAGNETIC FILLER'S IMPACT ON PEDOT/GRAPHENE COMPOSITE

E ASHOK SIVA KUMAR
Research Scholar Monad University, Delhi Hapur Road Village & Post Kastla, Kasmabad, Pilkhuwa, Uttar Pradesh
Dr. Satish Kumar
Research Supervisor Monad University, Delhi Hapur Road Village & Post Kastla, Kasmabad, Pilkhuwa, Uttar Pradesh

ABSTRACT
Microwave applications, a shielding material must have conductive and magnetic characteristics. Traditionally, heavy-weight magnetic/ nonmagnetic metallic materials were used as the shielding material which can be replaced by light-weight polymers and sp2 -hybridized carbon allotropes such as graphene, CNTs and fullerenes. Polyaniline composites with MWCNT, carbon fiber and graphene possessing core-shell morphology have been reported to have EM shielding effectiveness of 37, 31 and 39 dB respectively in the Ku frequency band. The graphene incorporated composite demonstrates better shielding result as compared to other fillers due to moderate electrical conductivity and large surface area. In case of metallic conductors, the shielding mainly dominated by reflection, and the reflected wave can still interact with other devices. As the electromagnetic wave absorption is related to the losses in the materials, magnetic materials such as soft ferrite and ferrite composites are widely used in shielding applications. At higher frequencies, these materials cannot function as good microwave absorbers because the permeability of these materials decreases due to the eddy current losses induced by electromagnetic waves. As the natural resonance frequency of uniaxial anisotropic materials is proportional to their anisotropy fields, it is possible to use hard ferrites and their composites having large anisotropy as a microwave absorber. Strontium hexaferrite (SrFe12O19) is one such example with wide applications such as magnetic storage media, permanent magnets and microwave absorber being chemically inert, with large magnetization, anisotropic properties and having high frequencies response. Recently, Strontium hexaferrite (SrF) has been reported with promising microwave absorbing characteristics due to a high magnetic loss in high-frequency band, but high density and corrosion sensitivity limit its application.

KEYWORDS: Magnetic Filler, PEDOT/Graphene Composite, Microwave applications, shielding material, magnetic characteristics, heavy-weight magnetic, nonmagnetic metallic materials

INTRODUCTION

As reported in several cases, the magnetic losses can be enhanced by incorporating ferrite particles in the polymer matrix. It may also be observed that core-shell morphology of composites shows better EM

International Journal for Innovative Engineering and Management Research
PEER REVIEWED OPEN ACCESS INTERNATIONAL JOURNAL
www.ijiemr.org

shielding effectiveness due to their confinement effects, interfacial polarization, and synergetic behavior. Zhang et al. reported RGO/MnFe2O4/PVDF composites with a frequency range of 2-18 GHz having the minimum reflection loss of −29 dB at 9.2 GHz which is attributed to the dielectric loss, magnetic loss and the synergetic effect among the material. In this chapter, the effects of magnetic particles on magnetic, dielectric and microwave absorption properties of polymer nanocomposites have been investigated. Strontium ferrite nanoparticles along with RGO have been incorporated in PEDOT matrix using emulsion polymerization technique leading to the formation of PEDOT/RGO/SrF nanocomposites. The synthesis process allows the composites to gain core-shell morphology which has been confirmed by HRTEM. The synergic effect of the polymer, graphene and magnetic filler (SrF) is quite critical for EM shielding property of a material. The core-shell structured PEDOT/RGO/SrF (PSrG) nanocomposites of the conjugated polymer are expected to have prominent microwave absorption properties due to impedance matching and magneto-dielectric losses. With this objective, the effect of magnetic filler on the EM wave absorption properties of composites in high-frequency range has been studied and the impact of morphology and magnetic nature of composites is presented.

Experimental Section

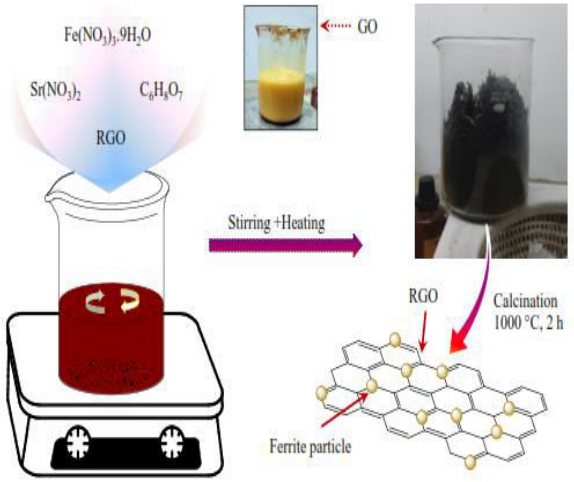

Figure 1: Schematic representation of the synthesis process of SrFe12O19/RGO (SrG) composites.

The reduced graphene oxide (RGO) has been synthesized. The RGO@SrF (SrG) composites filler were prepared via precursor method. In brief, the desired weight ratio of RGO was mixed with the stoichiometric ratio Sr(NO3)2 and Fe(NO3)3.9H2O in double distilled water. With constant stirring, citric acid was added to the above solution. The solution was evaporated at 90 °C under continuous stirring to form a viscous gel. Ammonia solution was added dropwise to maintain the pH of the solution at 8. The gel so formed was dried at 100 °C until it ignited in air. With citric acid as reductant and nitrates as oxidant, the gel gets burned to form dendrite-like structure which was then crushed to powder in a pestle mortar. The precursor consisting of oxides and carbonates further calcined at 1000 °C for 2 h resulting in the formation of strontium ferrite decorated RGO composite. Similarly, various compositions of RGO@SrF have

International Journal for Innovative Engineering and Management Research
PEER REVIEWED OPEN ACCESS INTERNATIONAL JOURNAL
www.ijiemr.org

been synthesized as listed in Table 1. The feed ratios of materials (PEDOT, RGO and SrFe12O19) are given in Table 1.

Table 1: Feed proportional ratio of the EDOT to feed ratio of Graphene to feed ratio SrFe12O19 and the labels assigned to different PEDOT/Graphene/SrFe12O19 nanocomposites.

Samples Name	Sample Weight Ratio		
	EDOT	RGO	$SrFe_{12}O_{19}$
PSrG1	1	0.5	0.5
PSrG2	1	0.5	0.9
PSrG3	1	0.5	1.3
PSrG4	1	0.5	2.2

RESULTS AND DISCUSSION

The nanocomposites of PEDOT/RGO/SrFe12O19 were prepared in a systematic way via in-situ chemical oxidative method doped with DBSA that also acts as a surfactant. In emulsion polymerization, EDOT monomer and SrF have been emulsified in an aqueous solution of DBSA resulting in the formation of micelles in which hydrophilic head of surfactant is outwards and hydrophobic tail shack towards micelles center. As shown in Figure 2, with the addition of initiator APS, polymerization began and polymer layers grow on SrG. The in-situ synthesis leads to the core-shell structure of composites and incorporation of RGO and SrFe12O19 contributes towards the dielectric and magnetic loss in order to achieve better shielding properties.

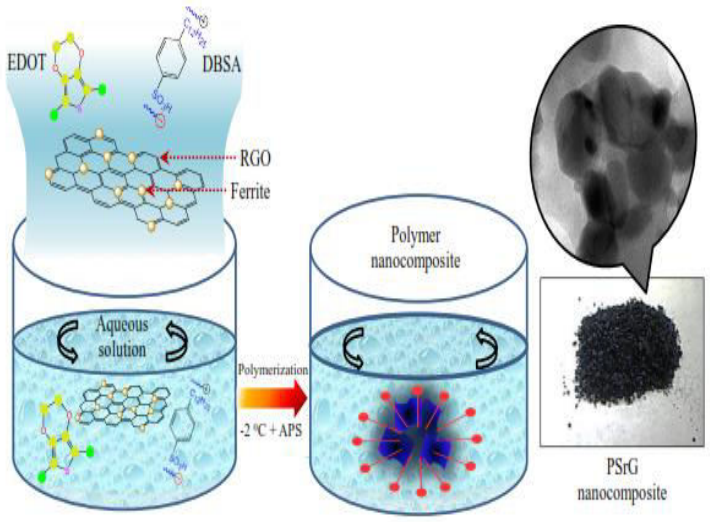

Figure 2: Scheme illustrates the various steps involve in the synthesis of PSrG nanocomposites.

1 Structural Investigation

The structure formation and surface morphology of graphene and PEDOT/graphene/SrFe12O19 composites were studied by using XRD, TEM, and FTIR techniques.

1.1 XRD Analysis

The X-ray diffraction pattern of PEDOT, SrF and PSrG composites is shown in Figure 3. It may be seen that the diffraction peaks corresponding to the (110), (008), (007), (114), (205), (217) and (2011) planes match well with the standard XRD data (JCPDS No.33-1340) of the face-centered cubic structured strontium hexaferrites and confirm the formation of SrF. The intensity of PSrG1 and PSrG4 is less than the pristine SrF sample. This may be due to the confinement effect of PEDOT matrix over the SrG material in the nanocomposites and also seen in the HRTEM image (Figure 4d). A hump seen in the XRD pattern of PSrG1 at 2θ from 19 to 27° gets shrunk in PSrG4

International Journal for Innovative Engineering and Management Research
PEER REVIEWED OPEN ACCESS INTERNATIONAL JOURNAL
www.ijiemr.org

due to high concentration of SrF in the nanocomposites. The small shift in the peaks corresponding to RGO and SrF fillers may be attributed to the interaction between the materials, perhaps due to the polar nature of materials.

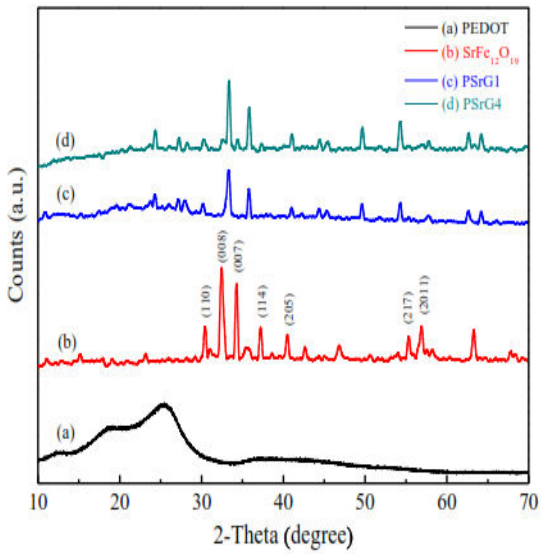

Figure 3: X-ray diffraction patterns of PEDOT, SrFe12O19 and PSrG composite.

1.2 HR-TEM Analysis

The morphology of as-synthesized RGO, SrG and PEDOT composites was studied using HR-TEM and corresponding micrographs are shown in Figure 4. As seen in Figure 4a, and its inset, thin and transparent sheets of RGO has been obtained from the reduction of GO with hydrazine hydrate. The RGO sheets appear as rippled or crumpled paper due to the deformation and restacking, as indicated by different brightness areas in the HR-TEM image. This intrinsic elastic nature of atomically thin 2-D RGO sheets may be expected to provide reasonable thermodynamic stability. The results of SrG in Figure 5.4b reveal that most of graphene surface is occupied by the SrF nanoparticles randomly dispersed and cross-linked with RGO sheets. Although, the sonication was performed during the samples preparation, nevertheless, the SrF nanoparticles get attached with the RGO sheets indicating adhesive bond established between the RGO and SrF nanoparticles. From inset of image (Figure 4b), lattice fringes corresponding to d-spacing, identify the presence of SrF nanoparticles over the RGO sheets. From the high-resolution TEM image of PSrG4 composite and corresponding magnified image, a large number of SrF nanoparticles of size 50-70 nm have been noticed in Figure 4c. Furthermore, the layout of amorphous PEDOT over the lattice fringes of SrG nanoparticles reveals that the polymer encapsulates both ferrite particle as well as graphene sheets resulting in the core-shell morphology as seen in Figure 4d.

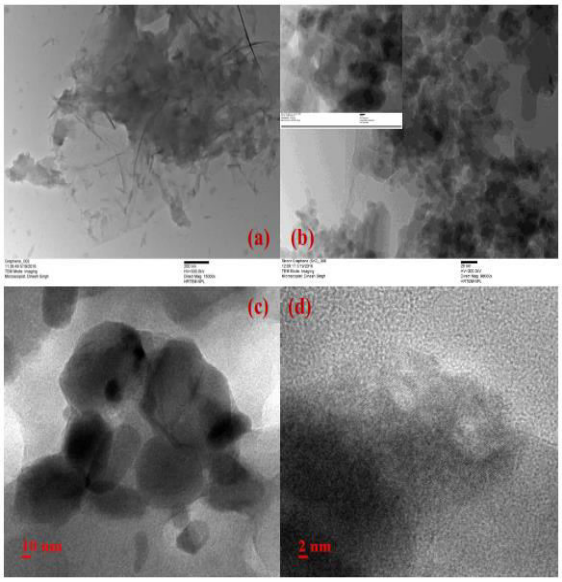

Figure 4: High-Resolution Transmission Electron Microscopy image of a) RGO, b) SrG (magnified image put in inset) C) PSrG4 and d) PSrG4 (magnified).

International Journal for Innovative Engineering and Management Research
PEER REVIEWED OPEN ACCESS INTERNATIONAL JOURNAL
www.ijiemr.org

1.3 FTIR Spectroscopic Studies

The reduction of graphene oxide and formation of PEDOT nanocomposites have been further investigated by identifying the peak of bonds of the materials using FTIR spectrograms as shown in Figure 5. The graphene oxide spectra shows the primary peaks at 1090 and 1727 cm-1 corresponding to epoxide (C-O-C) and carboxyl group (COOH) respectively, although the peak of some unoxidized graphite flakes may also be seen at 1621 cm-1 . On the other hand, after reduction of graphene oxide the peak of epoxide/carboxylic groups as disappeared or shrunk, thereby confirming the reduction of graphene oxide as shown in Figure 5a.

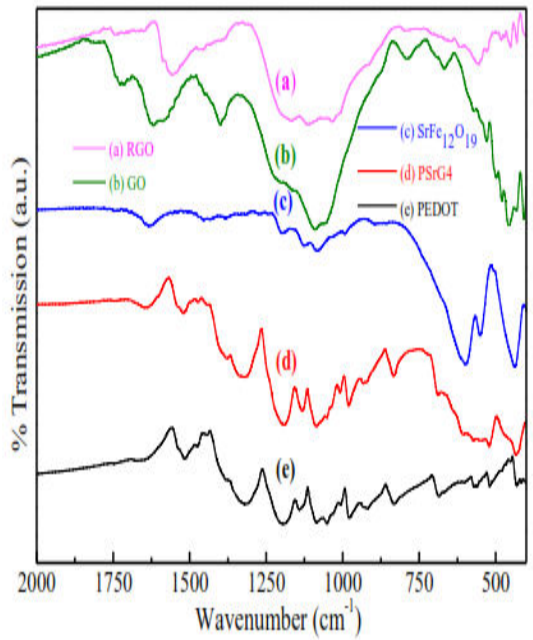

Figure 5: FTIR spectra of (a) RGO, (b) GO (c) SrFe12O19 (d) PSrG4 composite and (e) PEDOT. Plot (d) shows the absence of chemical bond formation between PEDOT, RGO and SrF.

In case of SrF, the absorption peaks observed at 603, 552, 434 cm-1 may be attributed to the asymmetric stretching and out of plane vibration of the octahedral and tetrahedral sites. In case of PEDOT (Figure 5e), the vibration bands corresponding to the thiophene ring stretching and C-C or C=C stretching of quinoid structure of thiophene ring are observed at 1517 and 1313 cm-1 respectively, whereas, the peaks corresponding to C-S bond of thiophene ring are observed at 978, 832 and 686 cm^{-1}. The spectra of PSrG4 composite as shown in Figure 5d depict various peaks of pristine materials (PEDOT, RGO and SrF) and absence of any unidentified peak. Thus, the stability of the polymer composites seems to increase due to compatibility between the polymer, RGO and ferrite. A small shifting in the absorption peaks of RGO and SrF present in the PSrG4 spectrogram may be due to the confinement effect of polymer, where solid-state charge transfer occurs between the electron deficient polymer and electron rich RGO sheets. Thus, intermolecular interaction occurring among the PEDOT/RGO/SrFe12O19 composites is helpful in enhancing microwave absorption properties.

2 Thermogravimetric Analysis

With a view to investigate the thermal stability of polymer composites, thermogravimetric analysis of PSrG1, PSrG2, PSrG3 and PSrG4 were carried out from room temperature to 700°C as shown in Figure 6A. Thermal stability of the PEDOT doped with DBSA was observed up to 220°C and above this temperature weight loss starts occur due to unbounded DBSA in the polymer matrix and further loss due to polymer degradation. In case of pure SrF, no

International Journal for Innovative Engineering and Management Research
PEER REVIEWED OPEN ACCESS INTERNATIONAL JOURNAL
www.ijiemr.org

weight loss is observed as it is already calcined at 1000°C. For PSrG composites, a weight loss of approximately 4% up to 120 °C may be due to the loss of water molecules entrapped in the polymer moiety for all samples. From 230-300 °C, the second weight loss seems to be due to loss of unbound/bounded dopant from the polymer matrix chain. This followed by third major weight loss in the temperature range of 400-550 °C was be due to degradation of polymer chains. It is further observed that the thermal stability of the composites increases with the concentration of SrF due to cohesive forces or ionic/Van der Waals forces between the various constituents (PEDOT, RGO, SrF) acting as a thermal barrier. The computed residue weight of PSrG1, PSrG2, PSrG3 and PSrG4 samples are 41%, 48.5%, 51.66% and 62.33% respectively at 700 °C mainly attributed to SrF and carbonaceous ash. The amount of residue weight also verifies the incorporated amount of SrF particles in the polymer matrix.

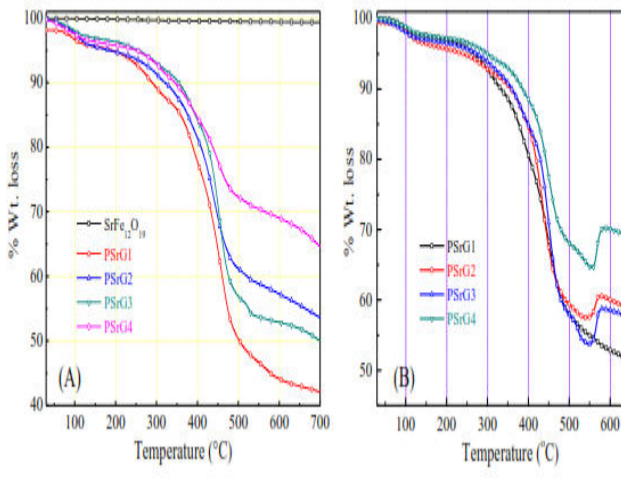

Figure 6: TG curves of A) PSrG composites and B) show the TG curves of the composites in the presence of magnetic field under N2 atmosphere.

To explore further, magnetic nature of the PSrG composites with temperature was investigated. The Curie point was determined by putting a small magnet over the TGA furnace during the measurement. On increasing the temperature, a point is reached where the ferromagnetic nature of PSrG composites changes over to paramagnetic materials. A sharp increase in the weight at 558 °C may be due to a change in the magnetic behavior of SrF as shown in Figure 5.6B.

3 Magnetic Studies

Figure 7A shows the hysteresis loops of the PEDOT composites incorporated with a different weight ratio of SrF at room temperature. The plots show a significant change in the saturation magnetization numbers, varying from 0.66131 to 8.60843 emu/g at 10K Oe and the values are given in Table 2. All composites show a significant change in the coercivity with the increase in the concentration of SrF. The coercivity is found to increase with SrF and PSrG4 has shown the maximum value of 5917 Oe. The remnant magnetization increases considerably with SrF concentration, and the highest remnant magnetization of 5.06 emu/g was observed in the PSrG4 composite. Thus, it can be noticed that the magnetic properties (coercive force, saturation magnetization and remnant magnetization) of the composites change significantly with SrF concentration. The confinement effect of non-magnetic polymer prevents the large aggregation of SrF nanoparticles resulting in the SrF particles

International Journal for Innovative Engineering and Management Research
PEER REVIEWED OPEN ACCESS INTERNATIONAL JOURNAL
www.ijiemr.org

arranged in a unified structure which leads the high magnetic polarization in accordance to the relation, where, $M_s = \phi m_s$ is saturation magnetization, ϕ is the volume fraction of the particles and ms is saturation moment of the single particle. An increased saturation magnetization (Ms) is normally advantageous for high permeability that contributes to high magnetic losses in the material. Consequently, the content of ferrite nanoparticles increases the saturation magnetization and hysteresis loss in the composites which contribute to the microwave absorption properties of the composites.

Table 2: Comparison of magnetic properties of PEDOT composites.

Samples	Coercive force H_c (Oe)	Saturation magnetization M_s (emu/g)	Remnant magnetiz (emu/g)
PSrG1	257	0.66131	0.1862
PSrG2	2540	2.21682	1.1261
PSrG3	2914	4.08126	2.3064
PSrG4	5917	8.60843	5.0621

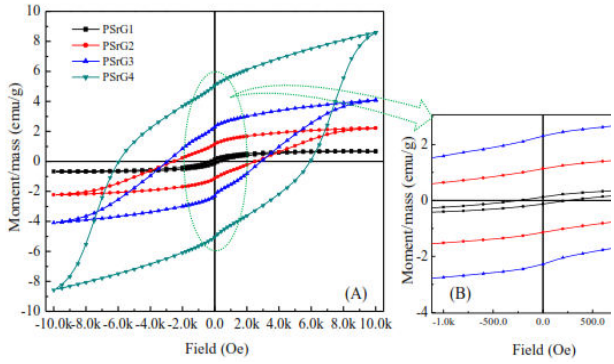

Figure 7: A) Magnetization curves of PSrG composites at room temperature and B) shows the zoomed magnetization curves at lower field.

4 Dielectric Studies

As discussed earlier, the attenuation of EM waves is associated with the dielectric and magnetic loss described in term of the frequency dependent relative complex permittivity (εr = ε' - jε") and permeability (μr = μ' - jμ"). These parameters have been calculated from scattering parameters (S21 and S11) based on the theoretical calculations given by Nicholson, Ross, and Weir method. The real & imaginary parts of complex permittivity & permeability represent the storage ability and energy dissipation capacity of EM waves respectively as shown in Figure 8. The variation of real (ε') & imaginary (ε") part of permittivity & permeability with frequency for PSrG1, PSrG2, PSrG3 and PSrG4 is shown in Figure 9A&B. As the dielectric parameters are mainly related with the polarization and conductivity of the material, various effects such as interfacial polarization, space-charge polarization, dipolar orientation polarization, electronic polarization and ionic polarization is frequency dependent. In the microwave frequency band, the real part of permittivity mainly correlated with the interfacial and space-charge polarizations. The contribution to the space charge and interfacial polarization add up due to the heterogeneity of the material. According to the Maxwell-Wanger polarization, the charge accumulates at the interface of two distinct materials due to the different conductivity and dielectric constant which further leads to interfacial polarization. In present case, the incorporation of SrF nanoparticles along with graphene in the conducting polymer

International Journal for Innovative Engineering and Management Research
PEER REVIEWED OPEN ACCESS INTERNATIONAL JOURNAL
www.ijiemr.org

matrix results in the formation of a heterogeneous system with more interfaces which lead to the attenuation of EM waves, and the attenuation is proportional to the square of EM wave intensity. It has been reported that the graphene and ferrite nanoparticles cause interfacial polarization and the coupling between them give rise to microwave absorption loss in the composite. Due to the different values of the dielectric constant and conductivity of PEDOT, RGO and SrF, some charge accumulates at their interfaces contributing to the interfacial polarization in the composites and hence increase the absorption of microwaves.

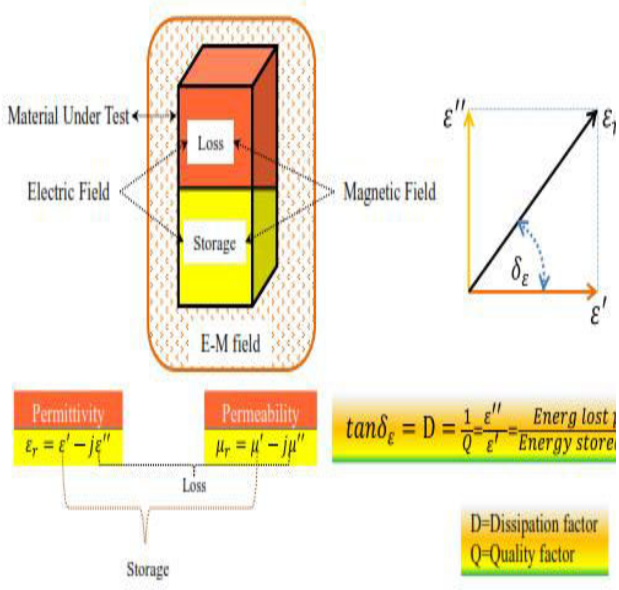

Figure 8: Schematic demonstration of electric and magnetic energy dissipation in the material.

In case of conjugated polymers, polarons (radical cations) and bipolarons (biradical cations) are the two types of charge species, move freely along the polymeric chains, whereas, bound charges (dipoles) have narrow mobility and are responsible for the strong dipolar orientation polarization in the composites. Thus the dipolar polarization may be related to the real part of permittivity. Since the PEDOT laminated SrF and graphene add up more conducting regions in the polymer matrix, in turn an increase in space charge polarization. The polarization being the function of frequency, the values of ε' & ε'' decrease as frequency increases, may be due to the decrease in dipolar orientation polarization as well as space charge polarization, with the increasing frequency as observed in Figure 9A. For PSrG composites at 12.4 GHz, the values of ε' vary from 14.8 - 23.0 and ε'' vary from 8.4 - 26.8. The complex permittivity increases with the concentration of SrF nanoparticle in the composites, primarily due to the formation of more interfaces within the composite. The synergic effect of SrF along with graphene and PEDOT results in higher microwave absorption. Figure 5.9B, depicts the variation of the real (μ') and imaginary (μ'') parts of the permeability with frequency in PSrG composites. As seen from the Figure, the real and imaginary parts of permeability decrease with increase in frequency and increase with the ferrite concentration. The maximum value of permeability has been observed in PSrG4 nanocomposite. The magnetic loss in the composites has been ascribed to the magnetic hysteresis loop, domain-wall resonance, magnetic resonance and eddy current phenomena of which the hysteresis, domain-wall resonance and eddy current loss may be mainly responsible in the microwave frequency range.

International Journal for Innovative Engineering and Management Research
PEER REVIEWED OPEN ACCESS INTERNATIONAL JOURNAL
www.ijiemr.org

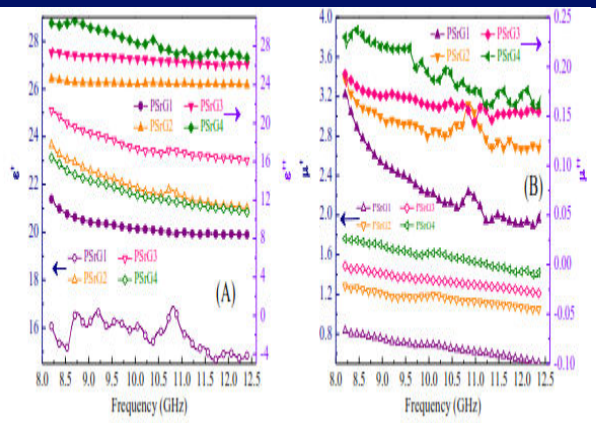

Figure 9: A) Behavior of real and imaginary parts of relative permittivity, whereas B) variation in real and imaginary parts of magnetic permeability.

For the hexagonal ferrites, the permeability can be defined as

$$\frac{(\mu-1)}{4\pi} = \frac{2M_S}{3H_A}$$

where HA is the anisotropy field and MS is the saturation magnetization. At lower frequencies up to critical frequency, the permeability remains equal to it dc (static) value and then starts declining with the increase in frequency. The higher value of static permeability leads to lower critical frequency as describe by Snoek‟s law. The frequency of this precession is governed by the coupling of magnetization with the c-axis. The stronger interaction leads to a higher natural frequency of precession. The strength of this interaction depends on the anisotropic field (HA) or magneto-crystalline anisotropy and is found to be higher for strontium ferrite. However, the imaginary part of permeability (μ′′) shows maximum power loss at resonance frequency. At high frequency, the magnetic dipoles attempt to swirl with the frequency however the induced field (M) straggled behind the magnetizing field (H) give rise to magnetic loss in the nanocomposites. The higher is the anisotropy more straggling will be produced results in enhanced magnetic losses. The magneto-crystalline anisotropy will be improved significantly with particle size, due to the microstructure defects and surface effect the smaller particle size of ferrite produce the larger specific surface area, and more regions are available for interaction with the electromagnetic wave resulting in higher dissipation of energy by the electromagnetic wave. In the present case, as may be seen from Figure 7, the saturation magnetization and hysteresis loss significantly increase with the increasing SrF particles concentration. Thus, the composites with a higher weight ratio of SrF, have a higher magnetic loss and show increased microwave absorption.

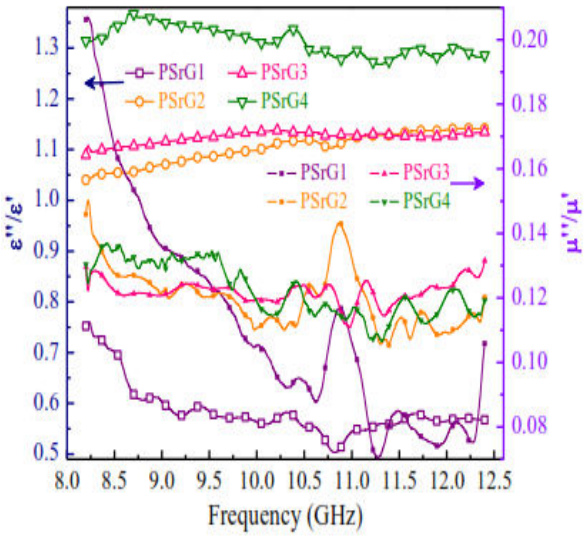

Figure 5.10: Variation in dielectric loss (tanδε = ε''⁄ε' and tanδμ = μ''⁄μ') with the frequency in 8.2 to 12.4 GHz.

International Journal for Innovative Engineering and Management Research
PEER REVIEWED OPEN ACCESS INTERNATIONAL JOURNAL
www.ijiemr.org

As already discussed, the attenuation of EM waves depends upon the relative dielectric and magnetic parameters of the material. To analyze the overall mechanism, the dielectric loss factor (tanδε = ε''⁄ε') and magnetic loss factor (tanδμ = μ''⁄μ'), with frequency are plotted in Figure 5.10. The maximum dielectric loss of 1.29 has been observed for the PSrG4 composite at 12.4 GHz revealing its lossy characteristics. On the other hand, as discussed above, the magnetic loss has also been found to increase with the concentration of SrF nanoparticles due to the increase in eddy current loss as well as hysteresis loss. Figure 5.11 shows the EM waves interaction with the material, showing various electric/magnetic phenomena in the material. The dielectric and magnetic loss in the 8.2- 12.4 GHz frequency range show better impedance matching properties in the composite resulting in good microwaves absorption properties originating from the synergic effect of PEDOT shell and graphene & strontium ferrite as cores.

CONCLUSION

The SEM and solvent extraction studies confirmed that PC/PP (60/40) blend has co-continuous morphology. A strong compatibilising action was noticed up on the addition of a small quantity of MWCNT into both dispersed and co-continuous morphologies. The size of the dispersed droplet was found to decrease linearly with the addition of the MWCNT followed by a leveling off at higher concentrations indicating interfacial saturation. This behaviour is analogous to the action of block and graft copolymers in incompatible polymer/polymer blends. A substantial refinement in the co-continuous structure was also observed with the addition of MWCNT as evidenced by the linear decrease of the wall thickness of both PC and PP phases followed by a clear leveling off indicating interfacial saturation. In other words, the addition of MWCNT into PC/PP co-continuous morphologies leads to a perfect interpenetration of both PC and PP phases. Interestingly, the addition of MWCNT increased the tendency for viscoelastic phase separation process due to the preferential migration of MWCNT to the PC phase. Theoretical predictions based on thermodynamic considerations clearly indicated the preferential localisation of MWCNTs in the PC phase. However, because of the viscosity differences between the two polymers, we also found that some of the MWCNTs being localised at the blend interphase and in PP phase as being evidenced by the high-resolution TEM data. The interface localisation leads to a decrease in the interfacial tension and increases in interfacial thickness. Therefore the observed compatibilising action could be explained as being due to: 1) the suppression of coalescence of the dispersed phase by the MWCNTs which act as a physical barrier against particle/particle agglomeration; 2). the decrease of interfacial tension by the localisation of the MWCNT at the blend interface. The addition of PP-g-MA into the PC/PP blend causes the refinement of the co-continuous morphology, decreased interfacial tension and suppression of coalescence. The co-continuous morphology

of PC/PP/PP-gMA has been unchanged by the inclusion of MWCNT.

REFERENCES

[1] A. De, P. Sen, A. Poddar, A. Das, Synthesis, characterization, electrical transport and magnetic properties of PEDOT/DBSA/Fe3O4 conducting nanocomposite, Synth. Met. 159 (2009) 1002–1007.

[2] Y. H. Kim, C. Sachse, M. L. Machala, C. May, L. Müller-Meskamp, K. Leo, Highly conductive PEDOT: PSS electrode with optimized solvent and thermal post-treatment for ITO free organic solar cells, Adv. Funct. Mater. 21 (2011) 1076–1081.

[3] G. A. Sotzing, K. Lee, Poly (thieno [3, 4-b] thiophene): a p and n dopable polythiophene exhibiting high optical transparency in the semiconducting state, Macromolecules. 35 (2002) 7281–7286.

[4] S. K. M. Jönsson, J. Birgerson, X. Crispin, G. Greczynski, W. Osikowicz, A. W. D. Van Der Gon, W. R. Salaneck, M. Fahlman, The effects of solvents on the morphology and sheet resistance in poly(3,4-ethylene dioxythiophene)/polystyrenesulfonic acid (PEDOT/PSS) films, Synth. Met. 139 (2003) 1–10.

[5] W. Zhang, B. Zhao, Z. He, X. Zhao, H. Wang, S. Yang, H. Wu, Y. Cao, Highefficiency ITO free polymer solar cells using highly conductive PEDOT: PSS/surfactant bilayer transparent anodes, Energy Environ. Sci. 6 (2013) 1956– 1964.

[6] A. M. Nardes, M. Kemerink, M. M. De Kok, E. Vinken, K. Maturova, R. A. J. Janssen, Conductivity, work function, and environmental stability of PEDOT: PSS thin films treated with sorbitol, Org. Electron. 9 (2008) 727–734.

[7] S. Kirchmeyer, K. Reuter, Scientific importance, properties and growing applications of poly(3,4-ethylene dioxythiophene), J. Mater. Chem. 15 (2005) 2077–2088.

[8] M. P. De Jong, L. J. Van Ijzendoorn, M. J. A. De Voigt, Stability of the interface between indium/tin oxide and poly(3,4-ethylene dioxythiophene)/poly (styrene sulfonate) in polymer light-emitting diodes, Appl. Phys. Lett. 77 (2000) 2255– 2257.

[9] D. Wakizaka, T. Fushimi, H. Ohkita, S. Ito, Hole transport in conducting ultrathin films of PEDOT/PSS prepared by layer-by-layer deposition technique, Polymer. 45 (2004) 8561–8565.

[10] W. N. York, Handbook of oligo and polythiophenes, Wiley-VCH, 1999. [41] T. S. Moss, M. Balkanski, Handbook on semiconductors, North-Holland, 1972.

[11] T. Kawai, T. Kuwabara, K. Yoshino, Electrochemical doping of conducting polymer in solution phase, Technol. Reports Osaka Univ. 41 (1991) 93–97.